Supporting Information

Hollow double-layer carbon nanocage confined silicon nanoparticles for high performance lithium-ion batteries

Jijun Lu[a,b,c], Dong Wang[a], Junhao Liu[a], Guoyu Qian[a], Yanan Chen[c,*], Zhi Wang[a,b,*]

[a] Key Laboratory of Green Process and Engineering, National Engineering Laboratory for Hydrometallurgical Cleaner Production Technology, Institute of Process Engineering, Chinese Academy of Sciences, Beijing 100190, P.R. China

[b] School of Chemical Engineering, University of Chinese Academy of Sciences, Beijing 100039, P.R. China

[c] School of Materials Science and Engineering, Key Laboratory of Advanced Ceramics and Machining Technology of Ministry of Education, Tianjin Key Laboratory of Composite and Functional Materials, Tianjin University, Tianjin 300072, P. R. China

E-mail: zwang@ipe.ac.cn; yananchen@tju.edu.cn

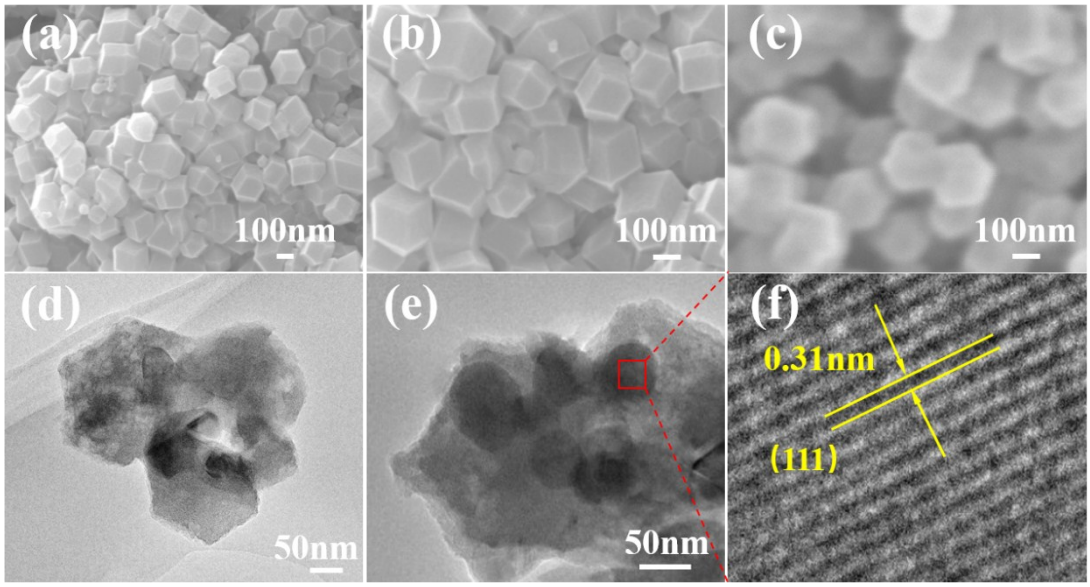

Fig. S1. (a, b) FESEM images of Si@ZIF-8; (c) FESEM images of Si@NC; (d, e, f) The HRTEM images corresponding to Si@ NC.

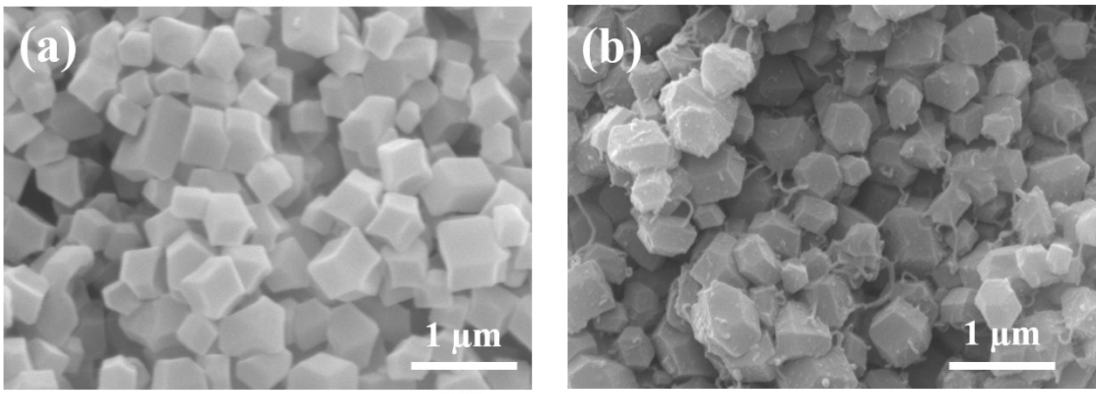

Fig. S2. (a,b) FESEM images of ZIF-8@ZIF-67 and H-NC@GC.

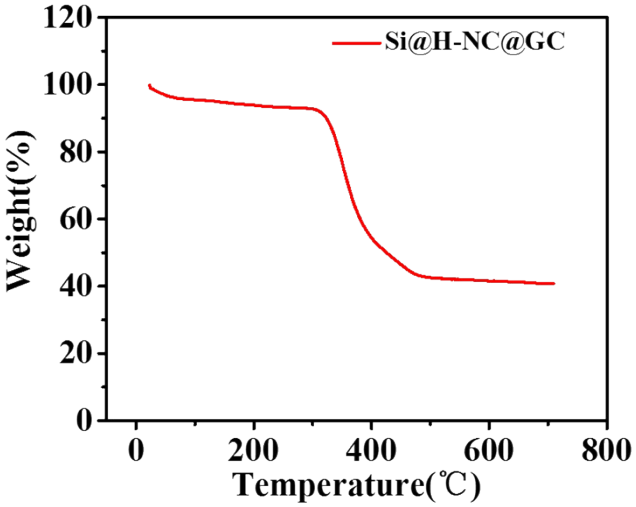

Fig. S3. TGA curves of the Si@H-NC@GC.

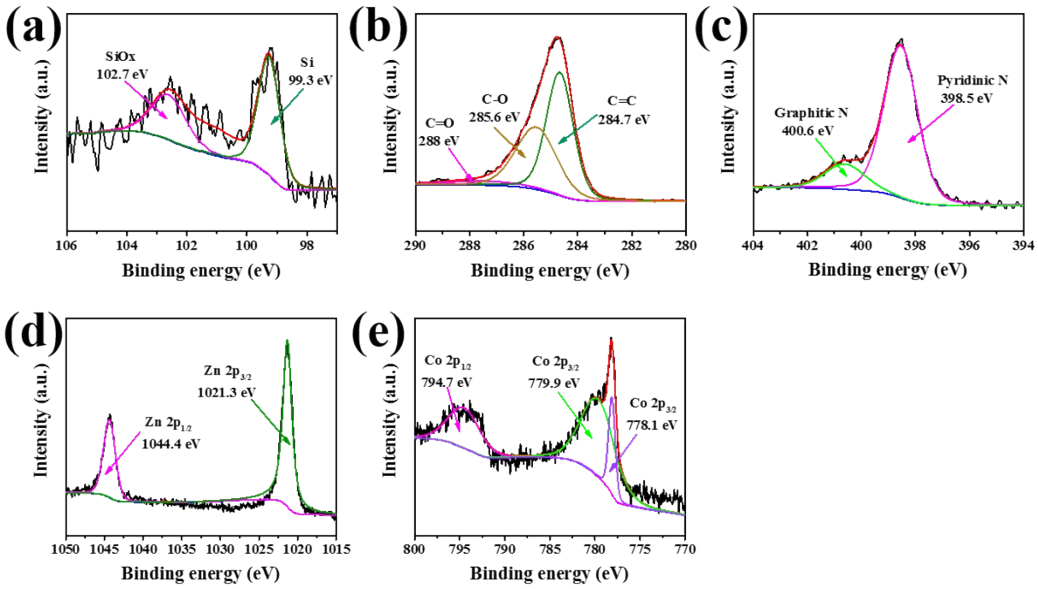

Fig. S4. XPS spectra of (a) Si 2p, (b) C 1s, (c) N 1s, (d) Zn 2p, (e) Co 2p of the Si@H-NC@GC sample.

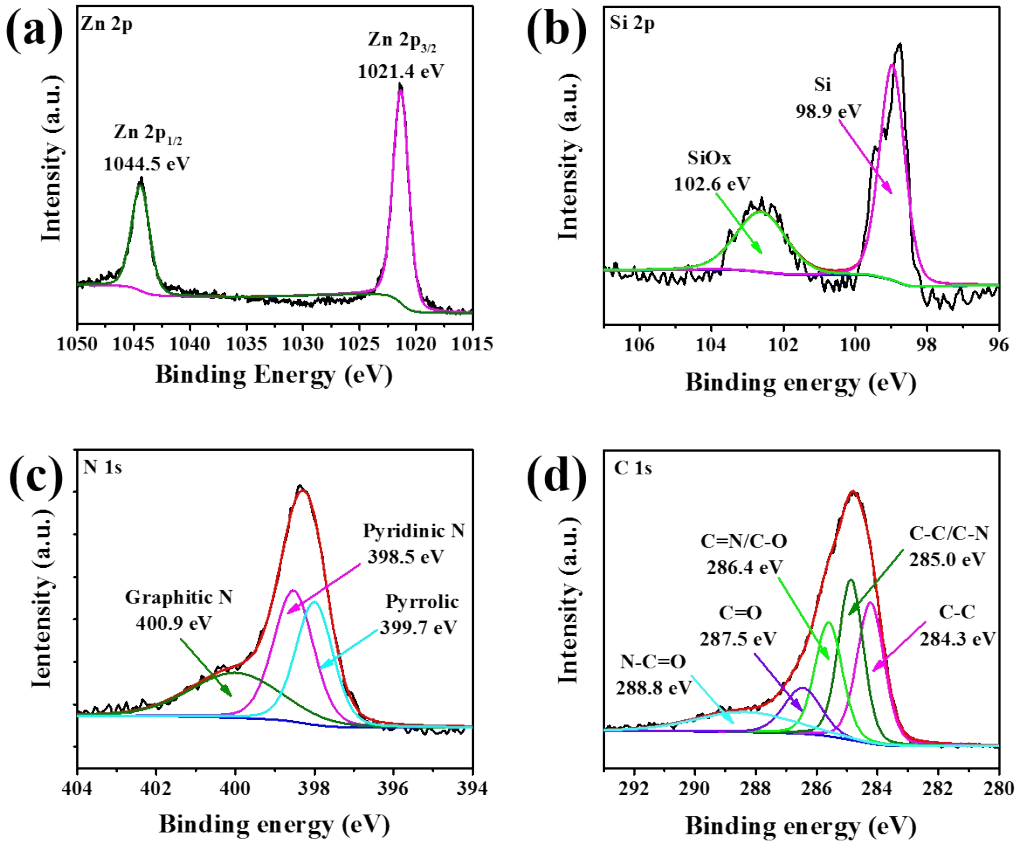

Fig. S5. XPS spectra of Zn 2p, Si 2p , N 1s, C 1s of the Si@NC sample. (a) Zn 2p has two peaks corresponding to metal Zn and ZnO at 1044.5 and 1021.4eV, respectively; (b) Silicon 2p has two peaks corresponding to silicon oxide and silicon at 102.6 and 98.9eV, respectively; (c) The N 1s peaks show the presence of pyridine N, pyrrole N and Graphitic N; (d) C1s peaks show N-doped carbon and carbon layers coating.

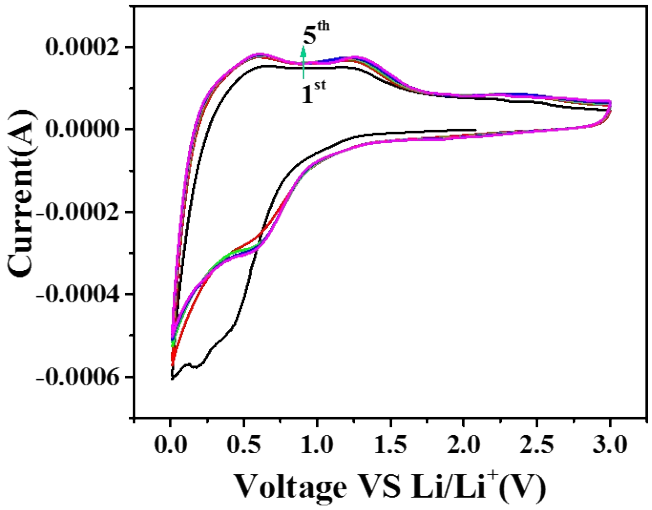

Fig. S6. CV curves for Si@NC at a scan rate of 0.5mV s^{-1} in the potential window of 0.01~3.0V vs Li/Li^+.

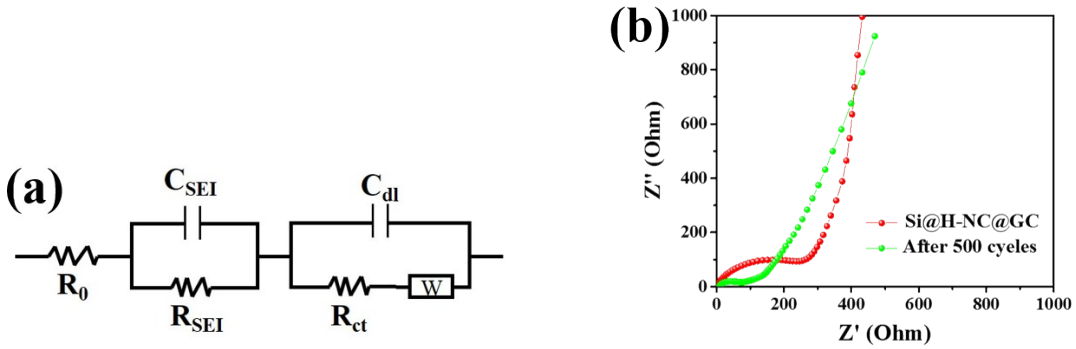

Fig. S7. (a) The corresponding equivalent circuit diagram of Si@H-NC@GC material EIS test; (b) Nyquist plots of Si@H-NC@GC composites before and after cycling.

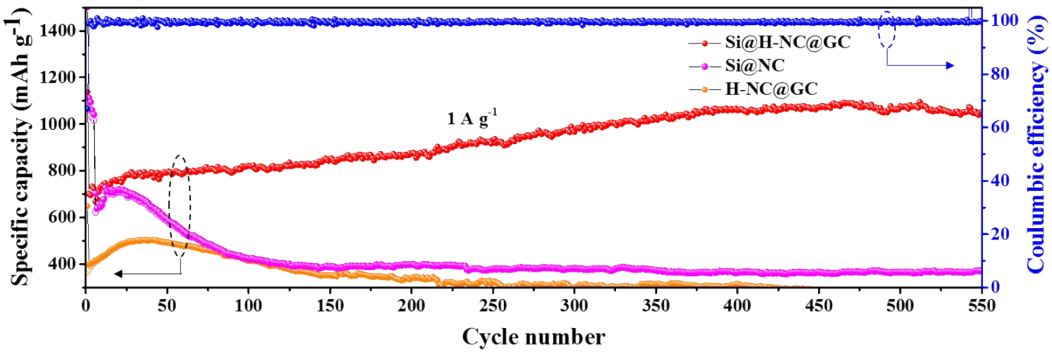

Fig. S8. Comparison of cycling performance of three electrodes at a current density of 1.0 A g^{-1}.

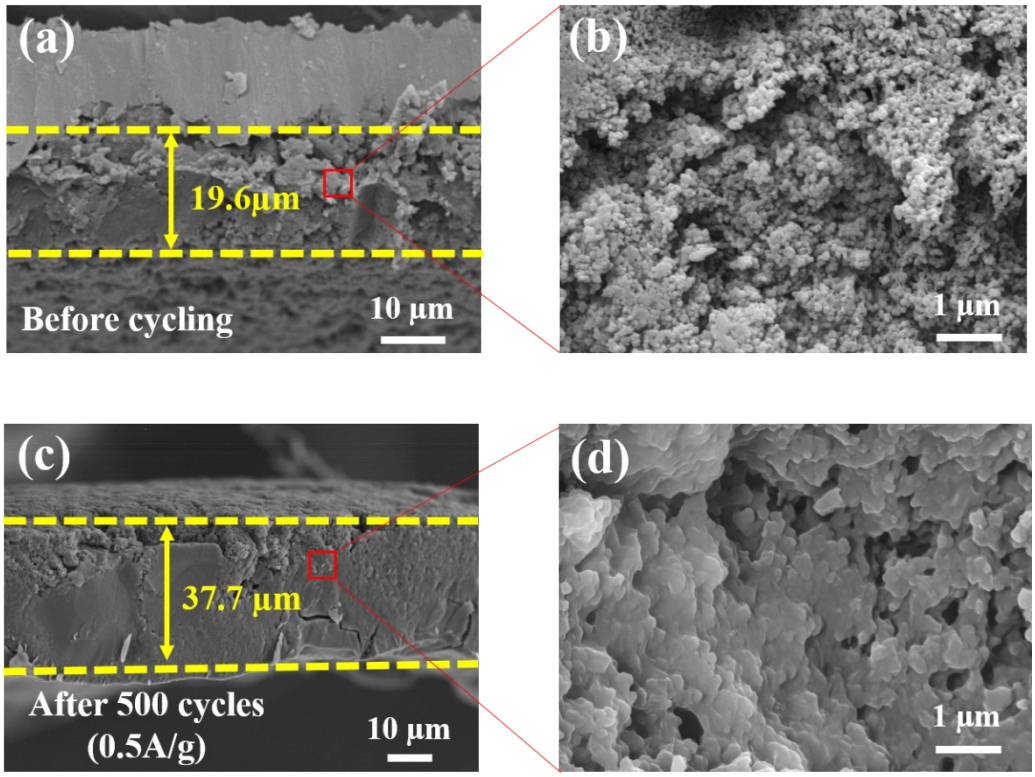

Fig. S9. (a) Cross-sectional SEM images of Si@NC; (b) Partial enlargement of active materials Si@NC electrode before cycling; (c) Cross-sectional SEM images of Si@NC electrode after 500 cycles at a current density of 0.5 A g^{-1}; (d) Partial enlargement of ctive materials Si@NC after 500 cycles.

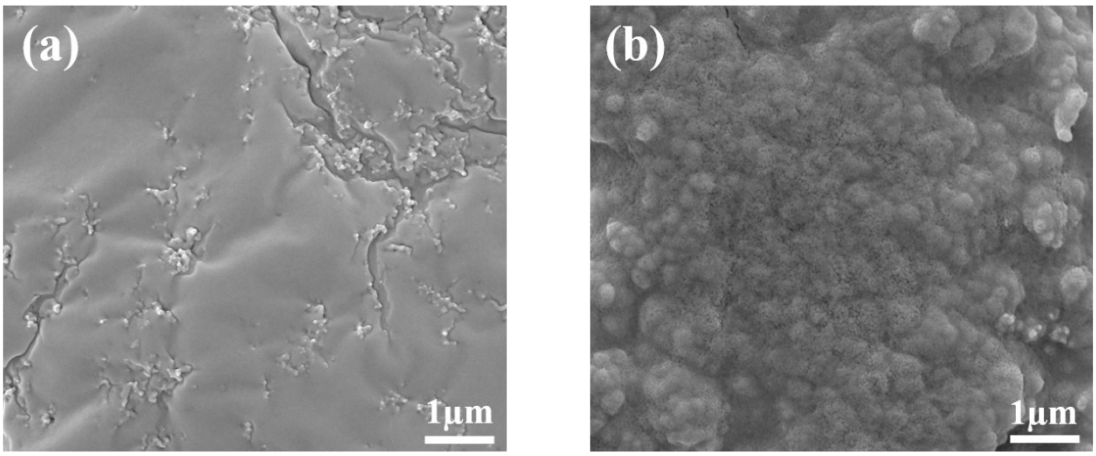

Fig. S10. (a) The electrode surface SEM images of Si@NC after 500 cycles at 0.5 A g^{-1} current density; (b) The electrode surface SEM images of Si@H-NC@GC after 500 cycles at 0.5 A g^{-1} current density.

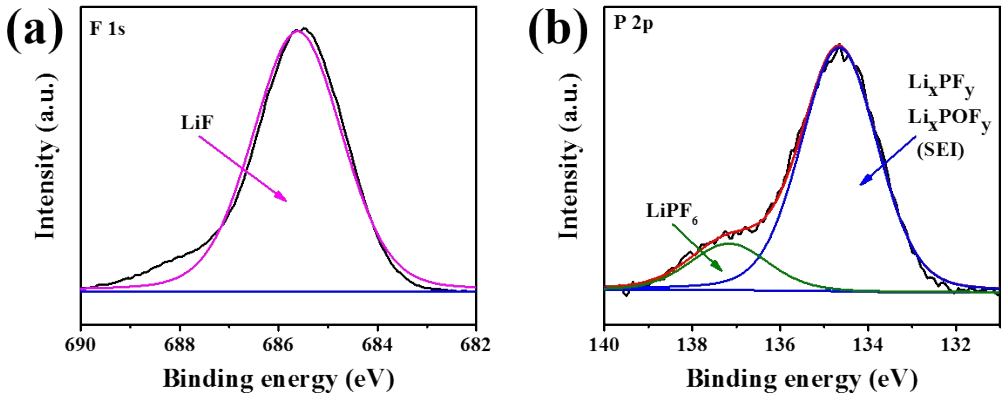

Fig. S11. XPS spectrum (a) F 1s, (b) P 2p of Si@H-NC@GC composite electrode after 400 cycles in $LiPF_6$.

Table S1. Performance comparison of present work with reported Si-based materials

Active material	Method	Current density (mA g^{-1})	cycles	Capacity (mAh g^{-1})	References
3D H-Macro-/Mesoporous Si	self-templated	200	300	959	[1]
Si@C@ZIF-67-800N	Self-templated	1000	300	852	[2]
Si/porous rGO composite	Template etching	50	100	1004	[3]
p-SiNPs@HC	Template etching	1000	600	600	[4]
P-Si/C	Electrospray	1000	120	979	[5]
Si/rGO/C	Freeze-drying and CVD	1400	300	840	[6]
yolk−shell Si/C	spray drying	100	100	934	[7]
SiNPs@rGO	self-assembly and Freeze-drying	500	200	880	[8]
Si@HC/CNFs	Electrospinning	200	100	1020	[9]
Si@SiOx@C	Pyrolysis	500	500	1030	[10]
Si@H-NC@GC	Self-templated	500 1000	500 550	1081 1053	This work

Reference:

[1] X.X. Zuo, Y.G. Xia, Q. Ji, X. Gao, S.S. Yin, M.M. Wang, X.Y. Wang, B. Qiu, A.X. Wei, Z.C. Sun, Z.P. Liu, J. Zhu, Y.J. Cheng, ACS Nano 11 (2017) 889-899.

[2] Y.C. Zhang, Y. You, S. Xin, Y.X. Yin, J. Zhang, P. Wang, X.S. Zheng, F.F. Cao, Y.G. Guo, Nano Energy, 25 (2016) 120-127.

[3] N.T. Liu, J. Liu, D.Z. Jia, Y.D. Huang, J. Luo, X. Mamat, Y. Yu, Y.M. Dong, G.Z. Hu, Energy Storage Materials 18 (2019) 165-173.

[4] S.C. Guo, X. Hu, Y. Hou, Z.H. Wen, ACS Appl. Mater. Interfaces 9 (2017) 42084-42092.

[5] G. Liang, X. Qin, J. Zou, L. Luo, Y. Wang, M. Wu, H. Zhu, G. Chen, F. Kang, B. Li, Carbon, 127 (2018) 424-431.

[6] K. Feng, W. Ahn, G. Lui, H.W. Park, A.G. Kashkooli, G. Jiang, X. Wang, X. Xiao, Z. Chen, Nano Energy, 19 (2016) 187-197.

[7] P. Guan, J.J. Li, T.G. Lu, T. Guan, Z.L. Ma, Z. Peng, X.Y. Zhu, L. Zhang, ACS Appl. Mater. Interfaces 10 (2018) 34283−34290.

[8] P. Chang, X.X. Liu, Q.J. Zhao, Y.Q. Huang, Y.H. Huang, X.L. Hu, ACS Appl. Mater. Interfaces 9 (2017) 31879−31886.

[9] Y.L. Chen, Y. Hu, Z. Shen, R.Z. Chen, X. He, X.W. Zhang, Y.Q. Li, K.S. Wu, Journal of Power Sources 342 (2017) 467e475.

[10] B.L. Jiang, S. Zeng, H. Wang, D.T. Liu, J.F. Qian, Y.L. Cao, H.X. Yang, X.P. Ai, ACS Appl. Mater. Interfaces 8 (2016) 31611−31616.